

Near-Earth Asteroid Missions Using Tether Sling Shot Assist

Eric L.-M. Lanoix* and Arun K. Misra†
 McGill University, Montreal, Quebec H3A 2K6, Canada

A new space exploration technique, called tether sling shot assist, is examined for near-Earth asteroid sample return missions. A spacecraft flying near an asteroid can attach itself to the asteroid using a space tether and an anchor device. After attachment, the velocity vector of the spacecraft relative to the asteroid can be rotated, thereby modifying its heliocentric velocity. The link to the anchoring device can then be severed, and the spacecraft can reel the tether back for reuse. A simplified analysis is presented of the problem, and the technical issues related to this maneuver are discussed. A trajectory analysis software is also developed and implemented to determine the possible trajectories of near-Earth asteroid sampling missions. For each trajectory, the strengths and weaknesses of different mission scenarios are highlighted. When combined with chemical propulsion, tether sling shot assist leads to very significant payload mass gains over conventional all-chemical propulsion systems.

Nomenclature

A	= tether cross-sectional area, m^2
a	= semimajor axis, m
\mathbf{a}	= acceleration vector, m/s^2
c	= characteristic speed of the tether material, m/s
e	= eccentricity
F	= thruster force, N
K	= maximum speed ratio during a tether sling shot assist (TSSA) mission, V_f^*/c
k	= number of periapsis passages between t_0 and t_f
L	= Lagrangian function of the spacecraft-tether system
l	= instantaneous tether length: distance between the spacecraft and the anchor point, m
l_0	= maximum tether length, m
M	= mean anomaly at epoch, rad
m_f	= fuel mass, kg
m_{ps}	= combined mass of the payload and probe structure, kg
m_{psf}	= combined mass of the payload, fuel, and probe structure, kg
m_t	= tether mass, kg
p	= semilatus rectum of an orbit, m
\mathbf{R}, \mathbf{r}	= position vectors, m
r	= variable of integration along the tether, m
r_a	= asteroid radius, m
S	= tether stress, N/m^2
S_0	= nominal tether stress, N/m^2
T	= tether tension, N
t	= time, s
\mathbf{V}	= velocity vector, m/s
v_0	= speed of the exhaust gases of a rocket engine, m/s
β	= flight-path angle during a TSSA, rad
Δ	= finite change in a quantity
θ	= true anomaly at epoch, rad
λ	= true longitude at epoch, rad
Π	= longitude of the periapsis, rad
ρ	= tether density, kg/m^3
ϕ	= swing-by angle, rad
ω	= sidereal rotational rate of the asteroid, rad/s

Subscripts

a	= asteroid
c	= chaser

f	= final or fuel
t	= target
tot	= total
0	= initial

Introduction

SENDING a spacecraft from one planet to another with the smallest amount of fuel has always been one of the fundamental problems of astronautics. Several orbital transfer and orbital maneuver techniques have been proposed and analyzed since the early part of the century. The simplest method for orbital transfer is the Hohmann transfer. Although very economical in theory, Hohmann ellipses require long transfer times and are not fuel efficient for high-energy missions. In such cases, they are often used in conjunction with gravity assist. However, the alignment of the planets required for gravity assist does not occur frequently.

The solar system holds millions of smaller bodies, such as asteroids. Using them as momentum sources would be advantageous over using heavy planets because of their great number. Approximately 2500 asteroids larger than 1 km (in largest dimension) orbit the sun along trajectories close to that of the Earth.¹ These objects are called near-Earth asteroids (NEAs). The close-range study of NEAs was the primary objective of the near-Earth asteroid rendezvous (NEAR) spacecraft.² NEAR flew by 253 Mathilde and 433 Eros and placed itself in an orbit around 433 Eros in February 2000.

None of these asteroids is massive enough to provide any significant gravity assist. However, a spacecraft flying near an asteroid can momentarily hook itself to the asteroid using an anchor device and a tether (Fig. 1). After attachment, the swing of the tether rotates the velocity vector of the spacecraft until it reaches the desired direction. If the link to the anchoring device is then severed, the spacecraft can reel the tether back for reuse, leaving the anchor on the asteroid. In this paper, the term tether sling shot assist (TSSA) designates this momentum change technique. The basic principle behind TSSA is that the tension in a space tether linking a spacecraft to an asteroid can transfer momentum, just as gravity does in gravity assist.

This technique was first proposed by Penzo and Mayer¹ and then studied further in Ref. 3. Puig-Suari et al.⁴ also studied the problem of tether assist, but in the context of catapulting payloads from a fixed launch platform on a planetary body. Yet much of their mathematical analysis also applies to TSSAs. Penzo and Mayer¹ derived the equations of tether tension and tether mass for a TSSA where the speed of the spacecraft with respect to the asteroid is constant. Penzo and Mayer restricted their analysis to uniform cross-sectional area and constant length tethers and proposed several applications of TSSAs. Lanoix³ also discussed the constant speed TSSA, but focused on the determination of the cross-sectional area, tether tension, and mass requirements for uniform stress tethers. Such tethers are tapered to maintain a uniform axial stress throughout the length of the tether. Finally, Ref. 3 provided estimates of the fuel savings

Received 4 January 1999; revision received 16 February 2000; accepted for publication 3 March 2000. Copyright © 2000 by the American Institute of Aeronautics and Astronautics, Inc. All rights reserved.

*Graduate Student, Department of Mechanical Engineering, 817 Sherbrooke Street West. Student Member AIAA.

†Professor, Department of Mechanical Engineering, 817 Sherbrooke Street West; misra@mecheng.mcgill.ca. Associate Fellow AIAA.

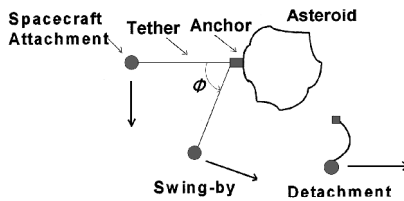


Fig. 1 Three phases of a TSSA.

involved with sending a spacecraft from the Earth to Jupiter using TSSAs on asteroids located in the main asteroid belt.

This paper extends on previous work on the TSSA maneuver (using a more in-depth but still simplified analysis) and presents the results of trajectory calculations performed using the actual orbital elements of 50 known NEAs. Payload mass optimization techniques are also developed. One particular mission scenario is studied: a multi-NEA exploration mission with sample return to Earth. This scenario serves as a basis for comparison between optimized TSSA spacecraft and conventional landing spacecraft relying on chemical propulsion.

The paper is divided into three main sections. First, the various stages of TSSA and conventional lander missions are discussed, and some of the technical problems related to each technique are identified. Second, all theoretical developments are presented. These include the equations of motion, as well as the equations governing tether tension and tether mass for the spacecraft-tether system around an asteroid. This section also contains all interplanetary trajectory calculations. Next, the results of the trajectory calculations performed for both optimized TSSA and conventional lander missions are presented. These results are then compared to determine which technique is more suitable for NEA sample return missions.

Mission Scenarios

Whether a conventional lander (with chemical propulsion) or a TSSA system is used to carry out the sample return mission, both types of spacecraft follow a similar trajectory around the solar system, only their asteroid rendezvous procedures differ. The first stage of both types of missions consists of launching the spacecraft from the Earth toward the first target asteroid. To simplify calculations, the patched conic method is assumed to apply.

The actual assist maneuver (for TSSA) begins once the spacecraft arrives near the asteroid. During the first step of the assist, the spacecraft hooks itself to the asteroid using the tether and an anchoring device (Fig. 1), for example, a penetrator. This operation is the most critical maneuver of the entire mission. Indeed, the spacecraft has to anchor an asteroid traveling at a relative speed of the order of 1–3 km/s using an anchor device located at the end of a 50–100-km-long tether. To prevent excessive tension immediately after attachment, the tether line must be nearly perpendicular to the surface of the asteroid at the instant when anchoring occurs.

During the second step of the assist maneuver, the swing-by, the spacecraft moves around the asteroid through some angle ϕ , like a pendulum (Fig. 1). This motion modifies the heliocentric velocity of the spacecraft. The assist continues until the swing-by angle ϕ reaches the value necessary to send the spacecraft to its next target.

Sampling occurs during the swing-by phase. For TSSA missions, the most effective way to sample the asteroid is to place the sampling mechanism in the anchor device. Once collected, the samples are transferred to a component of the anchor device designed to leave the asteroid with the tether at release. Taking the duration of a typical TSSA maneuver into account, the system would have about 1–4 min to carry out its task.

On the other hand, a conventional spacecraft must match the velocity of its target, land on it, and then use another thruster impulse to leave the asteroid and fly to its next destination. This operation requires a large amount of fuel. However, TSSA sampling probes do not suffer from this deficiency because they require little or no thruster impulse for sample collection.

The final phase of the assist maneuver, the detachment, occurs once the required swing-by angle has been reached. It consists of

cutting the link between the spacecraft and the asteroid at the anchor point (Fig. 1). The tether is then reeled back to the spacecraft for reuse. The reeling operation prevents the tether from being weakened or severed from micrometeoroid impacts, but it presents a major difficulty: increase in rotational rates. Because no appreciable external torque acts on the spacecraft-tether system after the detachment, the angular momentum of the system remains constant during tether retrieval. As the tether is reeled back, the moment of inertia of the system decreases. As a result, the rotational rate of the system may increase to high values. One of the possible solutions to this problem is to despin the system by applying a torque in the direction opposite to the angular momentum vector. This torque could be applied through thruster impulses.

After each assist or landing maneuver, both types of spacecraft travel from one asteroid to another until they reach the Earth. With proper guidance, little or no thruster impulse is needed at arrival near the Earth because the spacecraft is slowed by atmospheric friction. However, proper heat shielding is required to ensure payload survival during reentry.

Theoretical Considerations

Kinematics of a TSSA Maneuver

Because the main objective of this paper is to illustrate mathematically the potential of TSSA, the present analysis assumes that the spacecraft moves along the ecliptic plane and that the asteroid equator also lies along the ecliptic. Furthermore, the motion of the asteroid is assumed to remain unaffected by the maneuver. Indeed, the mass of the asteroid is so large compared to the combined mass of the spacecraft and tether that this assumption is quite valid, even though the principle of momentum conservation dictates a very slight change in the asteroid velocity following the assist.

During a TSSA, the system of interest consists of a spacecraft and a tether (Fig. 2). Although essential to the maneuver, the anchor device does not play any role in this simplified dynamical analysis because it is fixed to the asteroid. The spacecraft mass m_{psf} includes the payload, the probe structure, and the fuel contained in the spacecraft. At any instant, the tether has length l and mass m_t . The asteroid has radius r_a , and its sidereal spin rate is ω . The tether is deployed from the spacecraft, not from the anchor device.

Analyzing the motion of the system around the asteroid requires two reference frames: anchor point coordinates and asteroid-centered coordinates. The origin of the asteroid coordinate system ($O'X'Y'$) is the center of mass of the asteroid (Fig. 2). The $X'Y'$ plane spans the ecliptic plane, and the X' axis always points toward the vernal equinox. The Y' axis is oriented 90 deg counterclockwise with respect to the X' axis. The X' and Y' axes are hinged on the asteroid. As TSSAs occur over a short time compared to the orbital period of the asteroid, the velocity of the asteroid center of mass remains relatively constant during the TSSA. Therefore, the asteroid-centered coordinate system can be considered to be approximately inertial for this analysis. The anchor point coordinate system ($O''X''Y''$) has its origin at the anchor point (Fig. 2). The axes of this coordinate system follow the orientation of the tether at all times. Therefore, this coordinate system is not inertial. The swing-by angle ϕ denotes the angle swept by the tether since attachment.

The first step in deriving the equations governing a TSSA maneuver involves a kinematic analysis of the system. It is assumed that the tether is anchored near the equator of the asteroid and that the equator of the asteroid lies in the ecliptic plane. The inertial

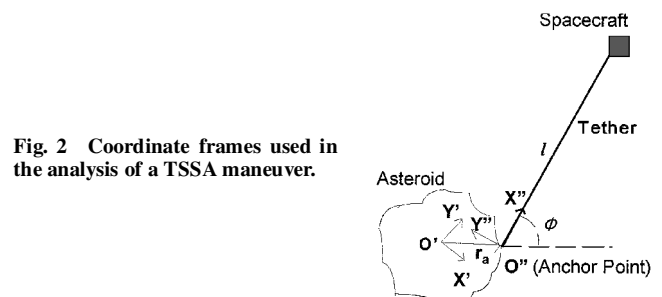


Fig. 2 Coordinate frames used in the analysis of a TSSA maneuver.

velocity and the acceleration of the spacecraft measured in anchor coordinates are given by

$$\begin{aligned} \mathbf{V}_s &= [\dot{l} + \omega r_a \sin \phi] \mathbf{i}'' + [(\dot{\phi} + \omega)l + \omega r_a \cos \phi] \mathbf{j}'' \\ \mathbf{a}_s &= [\ddot{l} - \omega^2 r_a \cos \phi - l(\omega + \dot{\phi})^2] \mathbf{i}'' \\ &\quad + [\omega^2 r_a \sin \phi + \ddot{\phi}l + 2\dot{l}(\omega + \dot{\phi})] \mathbf{j}'' \end{aligned} \quad (1)$$

where \mathbf{i}'' and \mathbf{j}'' are unit vectors in the X'' and Y'' directions, respectively. Similarly, the inertial velocity and acceleration of any tether element located at a distance r from the anchor point are given by

$$\begin{aligned} \mathbf{V}_r &= [\omega r_a \sin \phi] \mathbf{i}'' + [(\dot{\phi} + \omega)r + \omega r_a \cos \phi] \mathbf{j}'' \\ \mathbf{a}_r &= [-\omega^2 r_a \cos \phi - r(\omega + \dot{\phi})^2] \mathbf{i}'' + [\omega^2 r_a \sin \phi + \ddot{\phi}r] \mathbf{j}'' \end{aligned} \quad (2)$$

Note that the part of the tether from the anchor point to the spacecraft (the unreeled tether) does not move axially. Thus, r does not change with time, although l (the deployed tether length) does. Furthermore, the distance along the tether r is not to be confused with the distance between the asteroid center of mass and the anchor point r_a .

Dynamics of a TSSA Maneuver

The Lagrangian formulation is used to derive the equations of motion of the system (Fig. 2). In all practical cases, the gravitational attraction of the asteroid is negligible, and the tether has uniform density ρ . In what follows, l_0 is the total length of available tether. In other words, l_0 is the sum of the deployed and undeployed tether lengths. The cross-sectional area of the cable A may be a function of the position along the tether r . Finally, the spacecraft consumes fuel during the maneuver at a rate of dm_f/dt . With this in mind, the Lagrangian of the spacecraft-tether system swinging by an asteroid is

$$\begin{aligned} L &= \frac{1}{2} \left[m_{\text{psf}} + \rho \int_l^{l_0} A(r) dr - \int_0^{t_f} \dot{m}_f dt \right] [l^2 + l^2(\dot{\phi} + \omega)^2 \\ &\quad + \omega^2 r_a^2 + 2\dot{l}\omega r_a \sin \phi + 2\omega r_a l(\dot{\phi} + \omega) \cos \phi] \\ &\quad + \frac{\rho}{2} \int_0^l A(r) [r^2(\dot{\phi} + \omega)^2 + \omega^2 r_a^2 \\ &\quad + 2\omega r_a(\dot{\phi} + \omega)r \cos \phi] dr + \frac{\rho l^2}{2} \int_l^{l_0} A(r) dr \end{aligned} \quad (3)$$

The system has two degrees of freedom: the length of the tether l and the swing-by angle ϕ . The equations of motion of the system can be obtained using this Lagrangian, and they are

$$\begin{aligned} \left[m_{\text{psf}} + \rho \int_l^{l_0} A(r) dr - \int_0^{t_f} \dot{m}_f dt \right] [\ddot{l} - l(\dot{\phi} + \omega)^2 - \omega^2 r_a \cos \phi] \\ - \dot{m}_f [\dot{l} + \omega r_a \sin \phi] - \rho A(l) l^2 \\ = -T(l) + F_{x''} - \rho \dot{l} \int_l^{l_0} A(r) dr \end{aligned} \quad (4)$$

$$\begin{aligned} \left[m_{\text{psf}} + \rho \int_l^{l_0} A(r) dr - \int_0^{t_f} \dot{m}_f dt \right] \\ \times [\ddot{\phi} l^2 + 2\dot{l}(\dot{\phi} + \omega) + \omega^2 l r_a \sin \phi] \\ - \dot{m}_f [l^2(\dot{\phi} + \omega) + \omega l r_a \cos \phi] \\ + \rho \int_0^l A(r) [\ddot{\phi} r^2 + \omega^2 r_a r \sin \phi] dr = l F_{y''} \end{aligned} \quad (5)$$

where $F_{x''}$ and $F_{y''}$ are the thruster forces in the \mathbf{i}'' and \mathbf{j}'' directions, respectively.

Tension Expressions

Designing a tether strong enough to bend the trajectory of the spacecraft requires a knowledge of the variation of the stress S or tension T along its length. Applying Newton's second law in the \mathbf{i}'' direction on an infinitesimal tether element yields

$$\begin{aligned} (\mathbf{a}_r dm) \cdot \mathbf{i}'' &= \sum \mathbf{F}_{\text{ext}} \cdot \mathbf{i}'' = [T(r + dr) - T(r)] \\ &= [S(r + dr)A(r + dr) - S(r)A(r)] \end{aligned} \quad (6)$$

where \mathbf{a}_r is given by Eq. (2). Expanding the tether stress and cross-sectional area at $r + dr$ in a Taylor's series about r and neglecting terms of second and higher order in the Taylor expansions yields the tether tension equation

$$-\rho A(r) [r(\dot{\phi} + \omega)^2 + \omega^2 r_a \cos \phi] = A(r) \frac{dS}{dr} + S(r) \frac{dA}{dr} \quad (7)$$

To determine the tension/stress in the tether, an expression for $d\phi/dt$ is required. In all practical cases, the influence of the rotational rate ω of the asteroid on the behavior of the system can be neglected because the swing-by rate is two orders of magnitude faster than the asteroid rotational rate. If the tether remains completely deployed throughout the TSSA, that is, $d/dt = 0$, and if no thruster impulse is applied, that is, $dm_f/dt = 0$ and $F_{y''} = 0$, Eq. (5) yields

$$\dot{\phi} \left\{ \left[m_{\text{psf}} + \rho \int_l^{l_0} A(r) dr \right] l^2 + \rho \int_0^l r^2 A(r) dr \right\} = 0 \quad (8)$$

Because the quantity within the braces is nonzero, then the second time derivative of ϕ equals zero, or

$$\ddot{\phi}(t) = \text{const} \quad (9)$$

which means that the rotational rate and, hence, the linear speed of the spacecraft relative to the asteroid are constant. Penzo and Mayer¹ obtained a result identical to Eq. (9) by recognizing that, in this particular case, the tension force in the tether does no work on the system.

When a constant thruster pulse is applied in the plane of motion at an angle β with respect to the direction of motion, it can be shown that the swing-by rate $d\phi/dt$ depends on time in the following manner:

$$\begin{aligned} \dot{\phi}(t) &= \left\{ \dot{m}_f t v_0 \cos \beta + \dot{\phi}(0) l \left[m_{\text{psf}} + \frac{\rho}{l^2} \int_0^l A(r) r^2 dr \right] \right\} / \\ &\quad l \left[m_{\text{psf}} + \frac{\rho}{l^2} \int_0^l A(r) r^2 dr - \dot{m}_f t \right] \end{aligned} \quad (10)$$

where v_0 is the speed of the thrusters' exhaust gases. Determining the tension/stress at any point along the tether involves substituting the appropriate expression for the swing-by rate [Eq. (9) or (10)] into the tension equation [Eq. (7)] and then integrating the resulting equation. The following analysis considers two types of tethers: uniform area tethers and uniform stress tethers.

For a completely deployed uniform area tether, the second term on the right-hand side of Eq. (7) vanishes. Integration of the resulting equation (with $\omega = 0$) gives the tension at any point along the tether:

$$T(r, t) = S(r, t)A = [l\dot{\phi}^2(t)] [m_{\text{psf}} + (\rho Al/2)(1 - r^2/l^2)] \quad (11)$$

Equation (11) is a generalization of the result obtained by Penzo and Mayer.¹

The second case deals with a completely deployed uniform stress tether. For such tethers, the first term on the right-hand side of Eq. (7) vanishes, and the solution⁴ for the tension (with $\omega = 0$) is

$$T(r, t) = S(t)A(r) = [m_{\text{psf}} l \dot{\phi}^2(t)] \exp[\rho \dot{\phi}^2(0)(l^2 - r^2)] (2S_0) \quad (12)$$

where S_0 is the nominal tether stress. Equation (12) shows that, if the stress in the tether is to remain constant along the length, the tether must be tapered exponentially, with the thickest end of the tether at the attachment point.

Tether Mass Determination

The payload mass that can be sent on a TSSA mission strongly depends on the mass of the tether that must fly with the spacecraft. For constant length tethers, the required tether mass is a function of the maximum speed of the spacecraft relative to the asteroid, V_s^* . It also depends on a material property of the tether called characteristic speed c . The characteristic speed is a function of the design stress and the density of the tether material¹ ($c = [S_0/\rho]^{1/2}$). In most cases of interest, V_s is constant for a given TSSA maneuver. Because the maximum stress in uniform area tethers occurs at the anchor point ($r = 0$), Penzo and Mayer¹ used Eq. (11) to determine the required tether to spacecraft mass ratio for uniform area tethers as

$$m_t/m_{psf} = \left(1/K^2 - \frac{1}{2}\right)^{-1} \tag{13}$$

where K is the maximum speed ratio encountered during the mission (V_s^*/c). As expected, the tether-to-spacecraft mass ratio increases with increasing relative speed. However, Eq. (13) implies that uniform area tethers cannot resist the stress generated during a TSSA maneuver for which $K > \sqrt{2}$. Better results may be obtained with uniform stress tethers. The tether-to-spacecraft mass ratio for a uniform stress tether^{3,4} is given by

$$\frac{m_t}{m_{psf}} = K^2 e^{K^2/2} \sum_{n=0}^{\infty} \frac{(-K^2)^n}{2^n (2n+1)n!} \tag{14}$$

Figure 3 shows the tether-to-spacecraft mass ratio for both uniform area tethers and uniform stress tethers for various speed ratios. For low-speed ratios, the mass ratios are almost identical, but uniform stress tethers become more advantageous than uniform area tethers for values of K beyond 0.8. However, uniform stress tethers must necessarily be tapered and are, therefore, more difficult to manufacture than uniform area tethers.

Trajectory Analysis

This section describes the procedure followed to determine the trajectory of the spacecraft from one target asteroid to another and then back to the Earth at the end of the mission. The first part of this procedure consists of determining the points where any two coplanar and confocal orbits of any orientation intersect. Figure 4 shows this problem using the ecliptic coordinate system (OXY) centered on the sun. The algorithm is then applied to the problem of interest; that is, the interception of a target t by a chaser c moving in coplanar orbits around the sun.

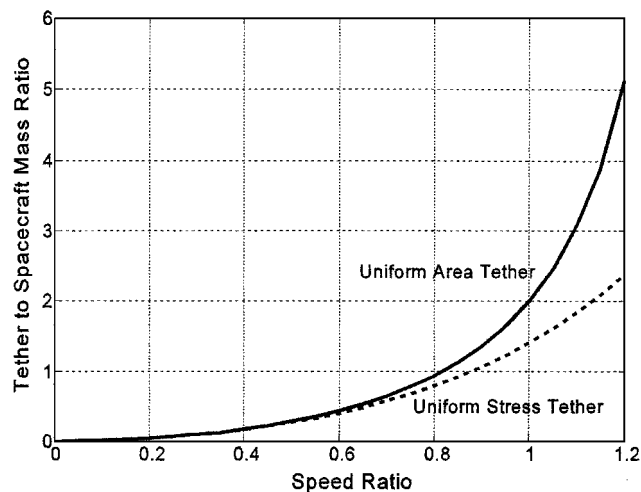


Fig. 3 Required tether to spacecraft mass ratio for the two different types of tethers.

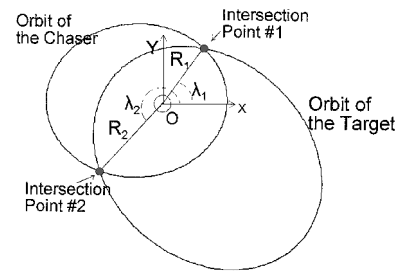


Fig. 4 Schematic representation of the intersection problem in ecliptic coordinates.

For the two orbits to intersect, the distance to the attractor R and the true longitude λ of both objects must match for some point(s). By using the equation of a conic in polar coordinates, these conditions can be written as

$$p_c/[1 + e_c \cos(\theta_c)] = p_t/[1 + e_t \cos(\theta_t + \Pi_c - \Pi_t)] \tag{15}$$

where p and e are the semilatus rectum and the eccentricity of the orbits, respectively, and the sum of the true anomaly θ and of the longitude of the periaapsis Π is the true longitude λ , that is, $\lambda = \theta_c + \Pi_c = \theta_t + \Pi_t$. In Eq. (15), θ_t was rewritten as $\theta_c + \Pi_c - \Pi_t$. The solution to Eq. (15) is given by

$$\theta_c = \arcsin \left\{ \frac{(p_c - p_t)}{\sqrt{p_c p_t}} \left(\frac{e_c^2 p_t}{p_c} - 2e_c e_t \cos(\Pi_c - \Pi_t) + e_t^2 \right)^{-\frac{1}{2}} \right\} - \arctan \left(\frac{p_t e_c - p_c e_t \cos(\Pi_c - \Pi_t)}{p_c e_t \sin(\Pi_c - \Pi_t)} \right) \tag{16}$$

Depending on the argument of the arcsin function, any two coplanar and confocal orbits may have from zero to two intersection points. Equation (16) applies to all types of conics: circles, ellipses, parabolas, and hyperbolas.

Adjusting the initial velocity of a chaser so that its orbit intersects that of the target is a necessary but not a sufficient condition for the celestial bodies to meet. The objects must also reach the intersection point at the same moment. This additional constraint on the interception of two bodies requires the solution of the so-called time of flight problem. By the use of the equation for the time of flight of a celestial body between any two points along its orbit,⁵ the time of flight problem can be written as an equation whose roots must be found. This equation is called the time of flight difference (TOFD) equation:

$$f_{\text{TOFD}} = \sqrt{a_t^3} \mu (2\pi k_t + M_{t_f} - M_{t_0}) - \sqrt{a_c^3} \mu (2\pi k_c + M_{c_f} - M_{c_0}) \tag{17}$$

where a is the semimajor axis of the orbit and μ is the gravitational parameter of the attractor. The mean anomaly is M . The solution to the interception problem requires a simultaneous solution to Eqs. (16) and (17).

Determination and Optimization of the Payload and Structural Mass

The following discussion assumes that the initial Earth departure boost is given to the spacecraft by an upper stage that is not considered as part of the spacecraft. For the conventional lander (using chemical propulsion only), the payload mass can easily be determined from Tsiolkovsky's rocket equation.⁶

As will be seen later, many practical cases of TSSA involve swing-by maneuvers at very high speed ratios. If the speed ratio exceeds $\sqrt{2}$, a uniform area tether cannot resist the resulting tension. To solve this problem, a payload mass optimization technique is used here and is shown schematically in Fig. 5. This procedure consists of firing the thrusters of the spacecraft just before any TSSA that would otherwise take place at a high relative speed. The lower relative speed of the maneuver decreases the required mass of the tether. After the TSSA, the thrusters are fired again to reaccelerate the spacecraft. This technique requires fuel, whereas an ordinary TSSA maneuver does not. Nevertheless, there exists a combination of fuel and tether

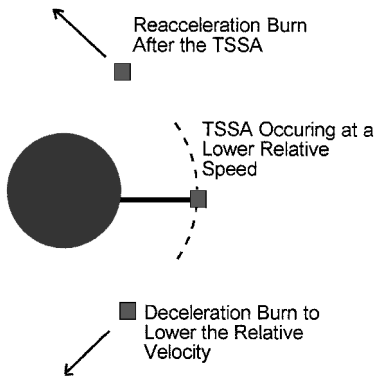


Fig. 5 Procedure for payload mass optimization.

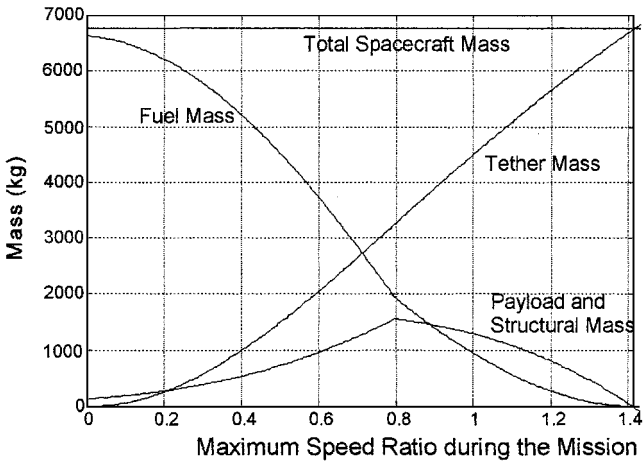


Fig. 6 Example of payload and structural mass as function of the allowable TSSA speed.

mass that maximizes the payload and structural mass. As will be seen later, this approach can substantially raise the payload and structural mass that can be sent on an NEA sample return mission.

To determine the optimized payload and structural mass of the probe, the trajectory of the spacecraft through the asteroids is first calculated using Eqs. (16) and (17). The interval of speed from zero to the largest TSSA relative speed encountered V_s^* is then divided into several subintervals. For a given relative speed within that interval, the required mass of the tether for every single TSSA is calculated using Eq. (13) or Eq. (14). The maximum tether mass for that relative speed is selected as the required tether mass. In this manner, the design tether mass for each relative speed is calculated. The amount of fuel required to achieve the prescribed relative speed and the allowable payload and structural masses are then obtained using Tsiolkovsky's law of rocket motion.⁶ Finally, the optimal spacecraft mass is obtained by sorting through all mass calculations from the subintervals and designating the largest value of payload and structural mass as optimal (Fig. 6).

Analysis and Results

The following analysis assumes that the Titan IVB launch system is used to place the interplanetary probe in a solar orbit.⁷ As for TSSA maneuvers, the candidate NEAs should have semimajor axes between 0.5 and 1.5 astronomical units, eccentricities below 0.5 and inclinations with respect to the ecliptic below 15 deg. These requirements are satisfied by 50 known NEAs, and their orbital elements can be found in the Steward observatory asteroid relational database.⁸ Required thruster impulses are assumed to be provided by an engine working with nitrogen tetroxide and monomethyl hydrazine ($N_2O_4 + MMH$). This oxidizer-fuel combination is commonly used for long-term missions.⁹ The speed of the exhaust gases for this type of engine is 3.14 km/s.

For TSSA missions, the anchor devices are regarded as probe structures. The tether material chosen for this analysis is Spectra, a highly oriented polyethylene fiber that has been used in several space tether experiments such as Small Expendible Deployer Sys-

tem (SEDS) and Tether Physics and Survivability (TiPS).¹⁰ The design characteristic speed of this material at low temperatures is 2.1 km/s, its density is about 970 kg/m³, and its safe working stress is 4.3 GPa (Ref. 11).

A MATLAB[®]-based trajectory and dynamical analysis software was developed to compute the parameters of the possible NEA sample return missions. The software assumes that, if a spacecraft can pass within 10,000 km of an asteroid, then the fuel expenditure required for interception is acceptable. A total of 61 distinct launch opportunities were found over a 25-year period starting on 1 January 2000, averaging almost two and one-half opportunities per year. Of these 61 trajectories, 67% could not intercept more than three asteroids. Nevertheless, one particular trajectory was found that would intercept as many as 16 asteroids.

Example of Payload and Structural Mass Optimization

Figure 6 shows a typical example of the payload mass optimization concept for a uniform area tether (UAT) TSSA mission. This particular example considers a mission for which the trajectory of the spacecraft intercepts three asteroids. As expected, the total spacecraft mass (6800 kg) is independent of the relative speed of the TSSAs and only depends on the ΔV required to place the probe into a solar orbit intercepting the first target asteroid. If no tether is used, the maximum speed ratio K for the mission is zero, and this case corresponds to a conventional lander mission. For such a mission, the probe and structural mass of the lander would be around 140 kg, compared to 6660 kg of fuel. The mass budget of an ordinary TSSA spacecraft is shown at the other end of the spectrum of relative speeds. Notice that, for this example, the maximum speed ratio is nearly equal to $\sqrt{2}$, the speed ratio for which the tether mass becomes infinite [see Eq. (13)]. For the maximum speed ratio case, the payload and structural mass of an ordinary TSSA spacecraft is nearly zero. The optimal configuration consists of swinging the spacecraft around the asteroids at a maximum speed ratio of 0.8. For this ratio, the tether and fuel masses would reach 3300 and 1950 kg, respectively. In the optimal case, the payload and structural mass would reach a maximum of 1550 kg, 11 times more than for the conventional lander. For all possible trajectories (not only for the 61 trajectories computed), the payload and structural mass of an optimized TSSA spacecraft is always higher than that of a conventional lander and that of nonoptimized TSSA spacecraft.

Payload and Structural Mass Budgets

Figure 7 shows the average payload and structural mass that can be sent on NEA sample return missions as a function of the number of asteroids encountered. For both a spacecraft equipped with a UAT and with a probe with a uniform stress tether (UST). For missions with less than five asteroids intercepted, the average payload and structural mass generally decreases as the number of asteroids encountered increases. This mass reduction is the result of an increase in the total propelled ΔV of the mission as the number of

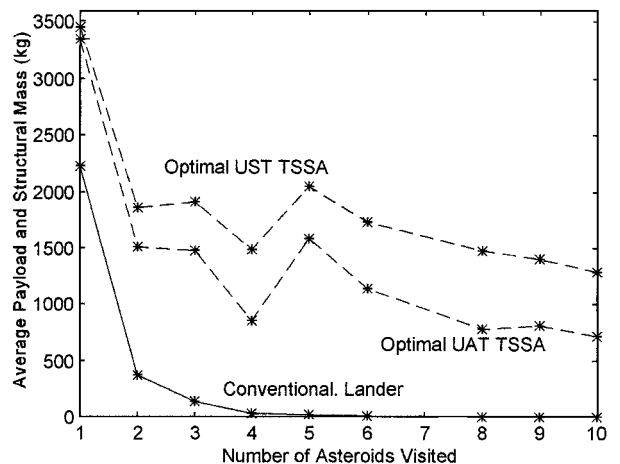


Fig. 7 Average payload and structural mass for a NEA sample return mission.

asteroids explored increases. By the use of Tsiolkovsky's rocket equation,⁶ this growth of the ΔV decreases the allowable payload and structural mass. As seen in Fig. 7, the exponential reduction in the payload and structural mass of the conventional lander is consistent with Tsiolkovsky's equation of rocket motion. Because of the small number of trajectories intercepting more than three asteroids, both TSSA curves behave erratically when more than three asteroids are sampled. The payload and structural mass carried by spacecraft intercepting 4–10 asteroids is probably constant near 0, 900, and 1500 kg for conventional, optimized UAT, and optimized UST spacecraft, respectively.

Given that a ΔV of 3.2–3.4 km/s is required to go from low Earth orbit to an NEA, the Titan IVB–Centaur Upper Stage combination can launch a spacecraft mass of 6600–6900 kg. For a conventional lander exploring two asteroids, the average payload and structural mass (371 kg) makes up less than 6% of the total spacecraft mass; the rest is fuel (Fig. 7). Because the mass of the thrusters and fuel tanks would likely exceed 371 kg, there would be absolutely no mass left for the payload.⁷ Therefore, this conventional NEA sample return mission is impossible. On the other hand, the mass of a conventional sampling spacecraft visiting only one asteroid averages 2230 kg: 34% of the total initial spacecraft mass. This ratio should be sufficient to allow a payload of a few hundreds of kilograms to carry out the sampling mission. Therefore, the highest average number of NEAs that a conventional spacecraft (using chemical propulsion only) can realistically sample during a mission is one.

The total fuel consumption of optimized TSSA missions usually does not exceed 1000–2000 kg. Although no detailed spacecraft design analysis was carried out, the mass of the tether management equipment, anchoring devices, fuel tanks, and thrusters are estimated to be under 400–500 kg. For all cases considered in Fig. 7, there would, therefore, remain enough mass for the sampling mechanism, collected samples, and the heat shield. Hence, NEA sample return missions exploiting trajectories intercepting from 2 to 10 asteroids cannot be carried out using a conventional lander, but it appears that these missions can be accomplished using an optimized TSSA spacecraft.

For missions designed to study more than one asteroid, the average optimized UAT and UST probes can carry 1040 and 1580 kg, respectively, more than the average conventional lander. Indeed, TSSA spacecraft need not land on and then takeoff from any of the asteroids that they sample. They merely anchor themselves onto the asteroids. Hence, tethered sampling spacecraft require a much smaller propulsive ΔV .

Conclusions

TSSA, a technique for NEAs sample return missions, has been examined. The results show that, on average, even the Titan IVB launch system cannot launch a chemically propelled lander capable of carrying out a sampling mission to more than one asteroid. This poor performance is mainly due to the amount of fuel required for ascent and descent in conventional sampling missions. However, optimized TSSA missions (relying on both TSSA and chemical propulsion) could be used to sample up to 10 NEAs per mission.

Although initial investigations show promising results, several technical problems must be overcome before any TSSA mission can be attempted. These include anchor device attachment and high spin rates during tether retrieval. These technical issues should be addressed in future investigations. Many possible applications of the TSSA concept remain to be explored. For example, other types of missions such as transferring heavy payloads to outer planets using TSSAs on main belt asteroids should be investigated.

Acknowledgments

This investigation was supported by the Natural Sciences and Engineering Research Council of Canada. In addition, the authors wish to express their gratitude toward the following people: Alexander Jablonski (Canadian Space Agency), James Harrison (NASA Marshall Space Flight Center), Joseph Carroll (Tether Applications), and Paul Penzo (Jet Propulsion Laboratory, California Institute of Technology). A preliminary version of the paper was presented as Paper AAS 97-604 at the AAS/AIAA Astrodynamics Specialist Conference, Sun Valley, ID, 4–7 August 1997.

References

- ¹Penzo, P. A., and Mayer, H. L., "Tethers and Asteroids for Artificial Gravity Assist in the Solar System," *Journal of Spacecraft and Rockets*, Vol. 23, No. 1, 1986, pp. 79–82.
- ²Farquhar, R. W., and Yeomans, D. K., "Waltzing by Mathilde: NEAR's First Asteroid Encounter," *Planetary Report*, Vol. 17, No. 2, 1997, pp. 4–8.
- ³Lanoix, E. L. M., "Tether Sling Shot Assists: A Novel Approach to Travelling in the Solar System," edited by K. Wong, *Proceedings of the 9th Canadian Aeronautics and Space Institute Conference on Astronautics*, Canadian Aeronautics and Space Inst., Ottawa, ON, Canada, 1996, pp. 62–71.
- ⁴Puig-Suari, J., Longuski, J. M., and Tragesser, S. G., "A Tether Sling for Lunar and Interplanetary Exploration," *Acta Astronautica*, Vol. 36, No. 6, 1995, pp. 291–295.
- ⁵Bate, R. R., Mueller, D. D., and White, J. E., *Fundamentals of Astrodynamics*, Dover, New York, 1971, p. 186.
- ⁶Tsiolkovsky, K. E., "Exploration of the Universe with Reaction Machines," *Exploring the Unknown*, Vol. 1, edited by J. M. Logsdon, NASA SP-4218, 1995, pp. 59–84.
- ⁷Loftus, J. P., and Teixeira, C. T., "Launch Systems," *Space Mission Analysis and Design*, edited by W. J. Larson and J. R. Wertz, Microcosm and Kluwer Academic, Torrance, CA, 1992, pp. 665–692.
- ⁸Univ. of Arizona, Steward Observatory Asteroid Relational Database (SOARD) [online database], telnet spider.aml.arizona.edu [cited 15 May 1997].
- ⁹Sackheim, R. L., Wolf, R. S., and Zafran, S., "Space Propulsion Systems," *Space Mission Analysis and Design*, edited by W. J. Larson and J. R. Wertz, Microcosm and Kluwer Academic, Torrance, CA, 1992, pp. 637–664.
- ¹⁰Cosmo, M. L., and Lorenzini, E. C., *Tethers in Space Handbook*, 3rd ed., Smithsonian Astrophysical Observatory, Cambridge, MA, 1997, pp. 15–20, 25–27.
- ¹¹Thompson, W. B., and Stern, M. O., "A Skyhook from Phobos to Mars," *Proceedings of the 4th International Conference on Tethers in Space*, NASA, Washington, DC, 1995, pp. 1737–1745.

C. A. Kluever
Associate Editor